Some Interior Observations of Southeastern Montana Hailstorms

DENNIS J. MUSIL, SUNDAR A. CHRISTOPHER, REGINA A. DEOLA, AND PAUL L. SMITH

Institute of Atmospheric Sciences, South Dakota School of Mines and Technology, Rapid City, South Dakota

(Manuscript received 22 May 1990, in final form 18 May 1991)

ABSTRACT

This study investigates some of the characteristics of the interior regions of several hailstorms penetrated by the armored T-28 aircraft during the 1981 CCOPE field project. The vertical wind data were analyzed to identify updraft and downdraft regions to facilitate the discussion of measurements made within the identified draft regions, such as draft sizes and speeds, cloud liquid water concentrations (LWC), turbulence, and hail.

Updrafts were more numerous than downdraft regions, tended to have greater horizontal extent and higher speeds, and were somewhat more turbulent. Significant correlations existed between peak vertical wind speeds and peak values of LWC or turbulence, as well as (for updrafts) between peak speed and draft size. Values of the LWC were generally quite low compared to adiabatic values, with the exception of two large severe hailstorms that may have had adiabatic updraft cores. The general characteristics of the hail observations, such as number and mass concentrations, maximum sizes, and locations within specific draft regions are discussed. Reflectivity gradients computed from radar measurements were compared with the hail observations from the two largest storms; the analysis shows that the hail tended to be located in high-reflectivity regions rather than in regions of high-reflectivity gradient. The data are discussed in terms of possible implications for numerical modeling of precipitation processes in convective storms.

1. Introduction

Vertical motions and cloud liquid water play integral roles in the development of precipitation in convective storms. For hailstones to develop, the updrafts must be strong enough that the incipient hail particles can remain aloft for a reasonable amount of time, while encountering an adequate amount of supercooled liquid (Dennis and Musil 1973). The processes necessary to accomplish this development are extremely complicated and not well understood, primarily because of a lack of understanding of the details and a scarcity of observations from within the storms.

Numerical models have provided a means of studying some of the details of the hailstone growth mechanisms. Specifications of vertical velocities and cloud liquid water concentrations (LWC) are critical to the results from most of these models; the models employ fields ranging from the idealized vertical air motions and LWC used by Musil (1970) and Dennis and Musil (1973) to the incorporation of two- and three-dimensional flow fields observed by Doppler radar (e.g., Paluch 1978; Heymsfield 1982; Miller et al. 1983; Nelson 1983; Foote 1984). These model studies typically treat the updrafts as containing some specified fraction of the adiabatic LWC (often 100%), while downdrafts are assumed to have no cloud liquid. Miller et al. (1988) have developed a somewhat more realistic incorporation of cloud liquid in their model by restricting the adiabatic values to regions with updraft speeds > 10 m s^{-1}. The coupled dynamic–microphysical model described by Farley and Orville (1986) may provide an even more realistic treatment of the development of cloud liquid water and the hailstone growth environment (see also Kubesh et al. 1988).

Despite the somewhat idealized nature of the flow and LWC fields often used, the models have been employed to study various aspects of the hail growth process. For instance, Dennis and Musil (1973) have shown that the maximum hailstone size is strongly related to the maximum updraft speed and the temperature at which it occurs. Heymsfield (1982) showed that hail could have developed in a storm from soaking of aggregates and graupel as they traveled along the southern periphery before finally growing to hail in and near the main updraft region of the storm. Nelson (1983) suggested that the horizontal size of the updraft region helps determine the sizes of hailstones; that is, wider updrafts are needed to produce larger hailstones.

The outputs from these and other models depend to varying degrees upon the specified conditions of vertical air motion and LWC. Knight and Knupp (1986) have shown that the results can be especially sensitive to the assumed specifications for the LWC. It is therefore worthwhile to investigate some of the in situ observations that are available from aircraft penetrations of hailstorms to compare the values used in the models against the observed data.

Corresponding author address: Dennis J. Musil, Box 318, Bayfield, WI 54814.

During the spring and summer of 1981, the field phase of the Cooperative Convective Precipitation Experiment (CCOPE) was conducted in southeastern Montana (Knight 1982). The overall objective of CCOPE was to develop an increased understanding of the precipitation mechanisms of convective clouds in the northern High Plains of the United States. One of the aircraft involved in these studies was the armored T-28 (Johnson and Smith 1980), which made numerous penetrations of thunderstorms during the field season. The T-28 provided a unique dataset related specifically to the hail growth problem. The microphysical instrumentation aboard the T-28 permits detailed observations of hydrometeors over almost the entire size spectrum, as well as other quantities of interest.

The purpose of this paper is to summarize the results of an investigation of the in situ measurements made by the T-28 during CCOPE. We endeavor to describe characteristic features of the group of storms observed, as opposed to concentrating on individual storms in a case-study mode. Initially, data from nine days with successful storm penetrations were considered for use in this study, but certain equipment malfunctions reduced the number of usable days for some analyses. For example, we desired to develop a dataset in which definitions of the vertical draft regions congruent with other earlier T-28 observations (e.g., Musil et al. 1977) could be made. However, draft regions could be identified on only seven of the days. Also, seven days had usable hail data, but only five days were common to both sets. Rather than limit the analysis to those five days, the seven suitable days were used for a general examination of conditions in the draft regions (section 4) and the different set of seven days was used for detailed analysis related to the hail observations (section 5).

2. Storm environments

The storms investigated could all be classed as mature thunderstorms/hailstorms. Table 1 shows information derived from rawinsondes taken in the inflow sectors of the storms penetrated by the T-28. In general, the sounding used was the last one taken prior to storm development; this was determined by noting the times when cumulus activity started, as well as the times when other project aircraft investigating the storms at an early stage of development departed the base at Miles City. The cloud-base parameters and the lifted-index values were obtained from parcel ascent by mixing the lowest 100 hPa of moisture. Using this procedure assumes that the storms were generated by surface heating, even though general dynamic and synoptic triggers such as short waves aloft, weak positive vorticity advection, or surface fronts are common in this area and were present on all of the days.

The storms experienced a wide range of instability, with lifted-index values between about −2° and −10°C. The storms on 1 and 2 August were particularly intense and contained some of the strongest vertical winds and highest liquid water concentrations ever observed with the T-28 system. The T-28 observations from the 1 August storm have been compared with two-dimensional (2D) cloud-model simulations (Kubesh et al. 1988) and used in an investigation of the role of melting and shedding in the production of hail embryos (Rasmussen and Heymsfield 1987). Miller et al. (1990) have given a detailed description of possible precipitation embryo sources and hail growth trajectories in the storm. The storm on 2 August formed the basis for a detailed investigation of microphysical characteristics in the weak-echo region (WER) of a supercell storm (Musil et al. 1986). A recent study by Miller et al. (1988) investigated the hail growth mechanisms for that same storm, but at an earlier time in its life cycle, using three-dimensional (3D) Doppler radar data.

Modeling studies by Weisman and Klemp (1982, 1984) showed that the dynamic characteristics of severe storms are partially determined by the relationship between buoyant energy and vertical shear of the horizontal wind. Following the methods of Rasmussen and Wilhelmson (1983), the values of shear below 4 km

TABLE 1. Airmass properties for selected CCOPE storms.

Date (1981)	Cloud base			Lifted index (°C)	Equilibrium level (km)	CAPE ($m^2 s^{-2}$)	0–4-km shear ($10^{-3} s^{-1}$)
	Height (km)	I (°C)	Mixing ratio ($g kg^{-1}$)				
12 July	3.8	6.0	9.5	−4	10.1	671	7.2
13 July	3.7	6.5	10.5	−3	12.3	1240	9.6
19 July	2.4	7.0	9.0	−2	10.2	306	7.2
21 July	3.6	2.0	7.1	−4	9.7	644	9.1
22 July	4.0	−2.1	5.3	−3	9.0	297	5.2
23 July	4.0	1.0	6.8	−5	10.3	750	6.6
29 July	4.0	3.2	8.2	−4	10.8	950	8.5
1 August	3.2	9.0	11.1	−9	11.4	2307	7.6
2 August	3.0	11.0	12.0	−10	11.9	3286	9.3

and convective available potential energy (CAPE) between cloud base and the equilibrium level, all shown in Table 1, were computed. The CAPE values were low, except for the extreme cases on 1 and 2 August. The shear values, which were calculated from the detailed wind profile, were all relatively high. No particular pattern emerges with respect to the 1 and 2 August cases, although they do fall in the tornadic region shown by Rasmussen and Wilhelmson, which is characterized by high shear and high potential energy. The remainder of the storms fall into the parameter space characterized by high shear and low potential energy.

3. T-28 data

This paper concentrates on conditions found in updraft and downdraft regions, as defined in section 3b. Variables investigated in those regions include the cloud LWC and turbulence, as well as the sizes and intensities of the draft regions. According to the flight plans devised for CCOPE, the T-28 penetrations were accomplished near an altitude of 6 km, corresponding to a temperature of about −15°C.

a. Calculations of vertical winds

The general form of the equation used for estimating the vertical air motions from the T-28 data is given by:

$$W_{ag} = W_{pg} + W_{ap}, \quad (1)$$

where W_{ag} is the vertical speed of the air relative to the ground, and W_{pg} and W_{ap} are the vertical speeds of the plane relative to the ground and of the air relative to the aircraft, respectively. Historically, the computation of vertical velocities using data from the T-28 system has been an evolving process using various equations derived from (1) as the instrumentation capabilities have improved.

Currently for the T-28, W_{pg} is calculated by converting pressure data from a static pressure transducer to altitude values and then differentiating with respect to time. The term W_{ap} has been the subject of much study and its determination has followed several approaches. These range from using empirical aircraft performance curves to account for the effects of changes in engine power (as represented by manifold pressure) and indicated airspeed (Auer and Sand 1966) to the development of simplifications to the airplane equations of motion. The latter has provided various approximations; one results from the substitution of changes in true airspeed in place of changes in ground speed to account for the effects of conversions between kinetic and potential energy of the aircraft (Dye and Toutenhoofd 1973; Cooper 1978). Another was provided by Kopp (1985), who modified the airplane equations of motion according to a method described by Kelly and Lenschow (1978) for inertial navigation systems (that modification being necessary because the T-28 has no such system). All of these methods assume that the horizontal wind is constant, since the T-28 has no way of measuring horizontal winds. This assumption may be questionable in a large thunderstorm, but Lenschow (1976) has shown that the effects of horizontal winds can be ignored in most cases. This seems valid considering that the T-28 objective is generally to identify the main draft regions of the storms.

Painstaking examination of results from the various methods available suggests that the Kopp method provides a smoother representation of vertical winds; the energy-balance approach seems to introduce a greater degree of roughness in the result. Furthermore, the Kopp method appears to handle the problem of pilot-induced response better. Consequently, the method of calculating vertical velocities used in this paper is that given by Kopp (1985). Unfortunately, the absolute accuracy of any of the methods cannot be well defined because no standard is available as a basis of comparison. The Kopp method is thought to give the most representative measurements of the main draft regions of the storms penetrated by the T-28 and should be accurate to within several meters per second, with a limiting response time of about 2–3 s.

Figure 1 shows an example of the calculated vertical wind, along with measured temperature and liquid water concentration. The wind calculation is still relatively noisy, even though a 9-s smoothing routine has been applied to the values. This particular penetration, which happens to contain the strongest updraft ever encountered with the T-28 (Musil et al. 1986), shows vertical wind speeds ranging between about +50 and −20 m s^{-1}.

b. Updraft and downdraft regions

Arbitrary criteria were used to define the vertical draft regions for each penetration for all days shown in Table 1 except 12 and 13 July. The data from those days suffered from anomalies in the pitch-angle observations, which resulted in uncertainties in the calculation of the Kopp vertical velocities. To be selected for the analysis, an updraft or downdraft had to occur continuously for at least 5 s of flight time (i.e., have a horizontal extent of at least 0.5 km) and have a peak speed exceeding about ±3 m s^{-1}, respectively, within the draft region. Thus, we are attempting to consider only draft-scale vertical motions, as this selection process eliminates small pockets of weak up- or downdrafts. No attempt is made to describe the rapid short-term gusts discussed by other investigators (e.g., Telford et al. 1977).

The method selected 113 updraft and 65 downdraft regions from the 19 penetrations on the last seven days listed in Table 1. Some examples of selected up- and downdraft regions are indicated in Fig. 1. The large updraft D was about 15 km in width, with a maximum speed > 50 m s^{-1}, while the adjacent down-

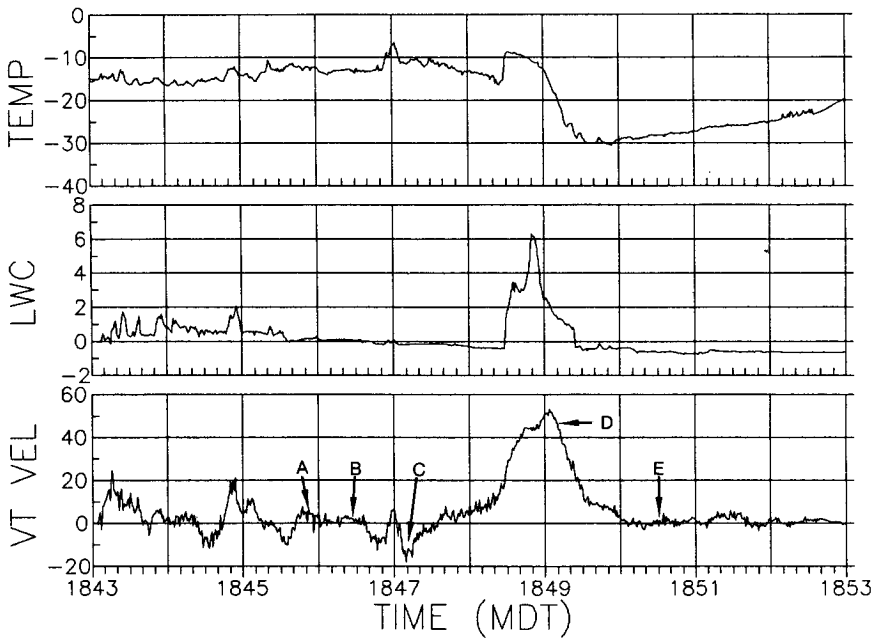

FIG. 1. Example of computed vertical wind velocity (m s^{-1}, lower panel) along with observed temperature (°C, top) and cloud liquid water concentration (g m^{-3}, middle) from penetration 1 of the 2 August 1981 CCOPE storm. LWC values <0 result from baseline drift in the Johnson–Williams device. Abscissa shows flight time (MDT); approximate conversion can be made to a distance scale by using the nominal true airspeed of 6 km min^{-1}. Letters indicate examples of identified updraft (A, B, D), downdraft (C), and quiescent (E) regions.

draft C approached 20 m s^{-1} and had a width of about 3.5 km.

Under these criteria, some updraft regions can include small, weak downdrafts and some downdraft regions can include small, weak updrafts. The strength of this scheme is that it can identify the main draft regions despite sometimes having small pockets indicating motion of the opposite sign (e.g., regions A and B in Fig. 1). These pockets may represent actual motions within the regions, but some result from uncertainties in the vertical wind calculations and others probably represent artifacts induced by aircraft or pilot responses. Often there are no indications of similar discontinuities in the other variables, and the process used prevents fragmentation of the penetrations into excessive numbers of small segments.

The scheme does not select certain quiescent regions of the penetrations (e.g., region E in Fig. 1), which are either too weak (do not satisfy the ±3 m s^{-1} restriction) or too narrow. About 60 such regions that could be visually identified in the plots were not selected as updraft or downdraft regions; they were generally small and represented about 24% of the total in-cloud observation time. Their possible role in the morphology of these storms is unknown and they were not considered in this analysis.

c. *Hydrometeors*

The T-28 can measure hydrometeors ranging from cloud droplets a few micrometers in diameter to hailstones several centimeters in diameter. A description of all the hydrometeor-sensing instruments can be found in Johnson and Smith (1980). In this section, the discussion is limited to the devices as they pertain to this study.

1) CLOUD-DROPLET SENSORS

Cloud liquid water concentration (LWC) was measured using both a Johnson–Williams (JW) sensor and a Particle Measuring Systems (PMS) forward-scattering spectrometer probe (FSSP). During CCOPE, the two devices tended to show reasonable agreement for values of LWC less than about 2 g m^{-3}. Figure 2 shows a sample comparison from a portion of the penetration shown in Fig. 1; in general, the two devices responded in a similar fashion, although the JW peaks were usually higher. Part of the difference shown appears to be due to the susceptibility for baseline drifting in the JW device.

The FSSP indicated much lower values when the LWC was higher. The exact reasons for this difference are unknown, but are probably related to the fact that

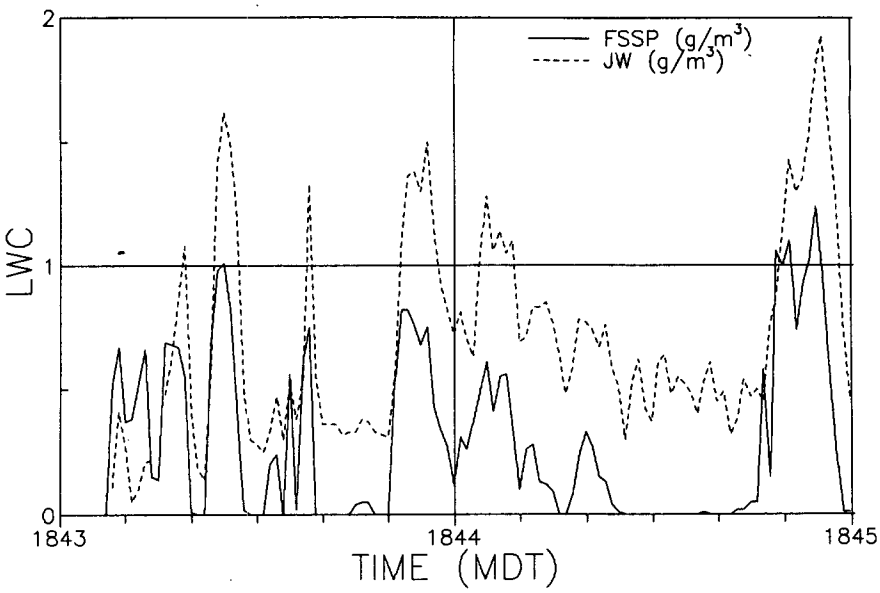

FIG. 2. Comparison of plots of liquid water concentration from the JW and FSSP devices from a portion of penetration 1 on 2 August 1981.

the FSSP suffers from saturation effects (Baumgardner et al. 1985). Without a means of investigating the problem further, it was decided to make a somewhat arbitrary "best estimate" of LWC from the two devices. Basically this meant that the JW was used for higher values, where it performed better than the FSSP. For lower values, FSSP observations were generally used because drifting in the JW observations caused more difficulties. Thus, it was not practical to use observations from one device on all the days. Moreover, absolute instrument accuracies are not well known, so the observations of LWC should be treated as estimates of the actual conditions found in these clouds. Nevertheless, the numbers are reasonable enough that relative comparisons can be made in the draft regions.

2) 2D-C PROBE AND FOIL IMPACTOR

Both the PMS 2D-C probe and the foil impactor can provide useful data on the precipitation particles ranging up to small hailstone sizes. However, the 2D-C probe did not provide reliable and consistent particle observations during all of the CCOPE penetrations by the T-28. The foil impactor (May 1974) was quite reliable, but the reduction of these data is tedious and time consuming. Consequently, only selected portions of the foil were analyzed by hand for use in specialized analyses of CCOPE data (Musil et al. 1986; Rasmussen and Heymsfield 1987; Kubesh et al. 1988). Since it was not possible to obtain comprehensive precipitation-particle data for all the previously defined draft regions, the approach in this study was to consider just those regions having common 2D-C and foil data in comparisons of the particle data.

Peterson (1989) has developed automated techniques for reducing the foil impactor data. These data have been extremely valuable in discussing various aspects of the precipitation mechanisms occurring in storms in the southeastern United States, where the particle shapes in the main draft regions are predominantly near spherical (Musil and Smith 1989; Peterson et al. 1990). However, the applicability of the techniques to foil data from High Plains storms with their preponderance of irregular ice particles is still being investigated.

3) HAIL SPECTROMETER

The T-28 hail spectrometer (Shaw 1974) is capable of determining number concentrations and size distributions of hailstones about 5–50 mm in diameter. It operates on a shadowgraph principle similar to that used in the PMS probes, with shadow sizes corresponding to particle sizes classified, counted, and recorded on magnetic tape for later analysis. The device appeared to work properly on all but one of the days shown in Table 1; malfunctions on 22 July negated the inclusion of that day in any hail analysis work. Also, no hail was encountered on 21 July. Both 12 and 13 July provided usable hail data but, as mentioned previously, the Kopp method for updraft calculation was not usable then due to other equipment malfunctions. Overall, the hail sensor provided a large sample of hail data on seven days for inclusion in this study.

d. Other observations

The T-28 system also measures the state variables, temperature, and pressure, as well as a number of vari-

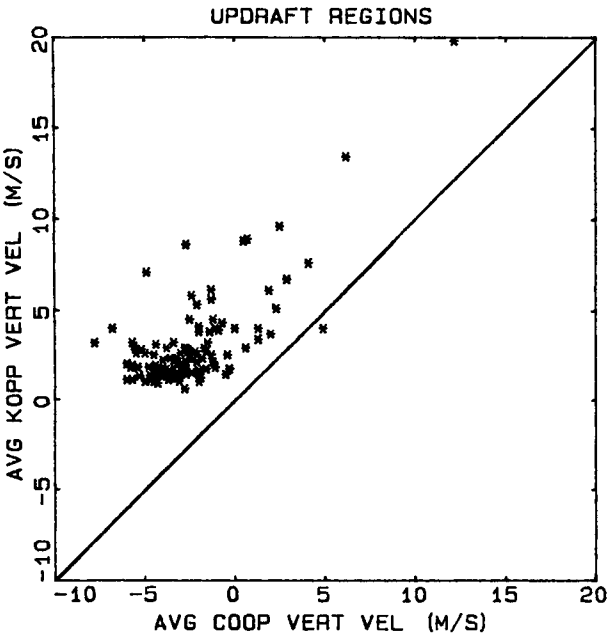

FIG. 3. Scatterplot comparing average vertical wind speed from the Cooper (abscissa) and Kopp (ordinate) calculation methods. Each point represents one of the 113 updraft regions identified using values from the Kopp formula. Diagonal line indicates 1:1 relationship.

ables related to aircraft navigation and performance. Many of them were useful in this analysis. Of particular interest are the calculated values of turbulence intensity; many hail suppression projects rely on the turbulence found in updrafts to disperse seeding material in the clouds where it may become effective in reducing hail. Little is known about the character of transport by the updrafts or the dispersion therein (see Stith et al. 1986), so knowledge of the turbulence in the vertical draft regions is desirable.

Turbulence intensity is calculated from the T-28 data by using the fluctuations in true airspeed over a selected time period (8 s in the CCOPE work) in a Fourier analysis. This results in a value for spectral energy that is related to the turbulent eddy dissipation rate ϵ (Sand et al. 1976). The values of turbulence intensity used in this study are actually the cube root of the energy dissipation rate (units of $cm^{2/3}\ s^{-1}$). In this form, the values can be easily compared with the descriptive categorizations by MacCready (1964).

4. Observations in the draft regions

More and larger updrafts than downdrafts were found in the Montana storms. The higher frequency of updrafts contrasts with other T-28 observations from storms in Colorado (Musil et al. 1977) and Alabama (Musil and Smith 1989). The reason for the apparent difference from Colorado to Montana is probably related to changing methods of determining vertical velocities over the years. Direct examination of this is not possible because of significant changes to the data system over time. However, a scatterplot (Fig. 3) comparing average vertical wind velocities from the Kopp and the previously used energy balance methods indicates fewer updrafts and a substantially greater number of downdrafts with the latter. The difference between the Montana and Alabama results is probably related to fundamental differences in the cloud and precipitation processes.

a. Draft sizes

The sizes of the vertical-draft regions defined in section 3b are shown in the frequency distributions in Fig. 4. The widths of the regions are represented as observed; it is not possible to determine the actual shapes of the regions or in what portions the aircraft actually flew.

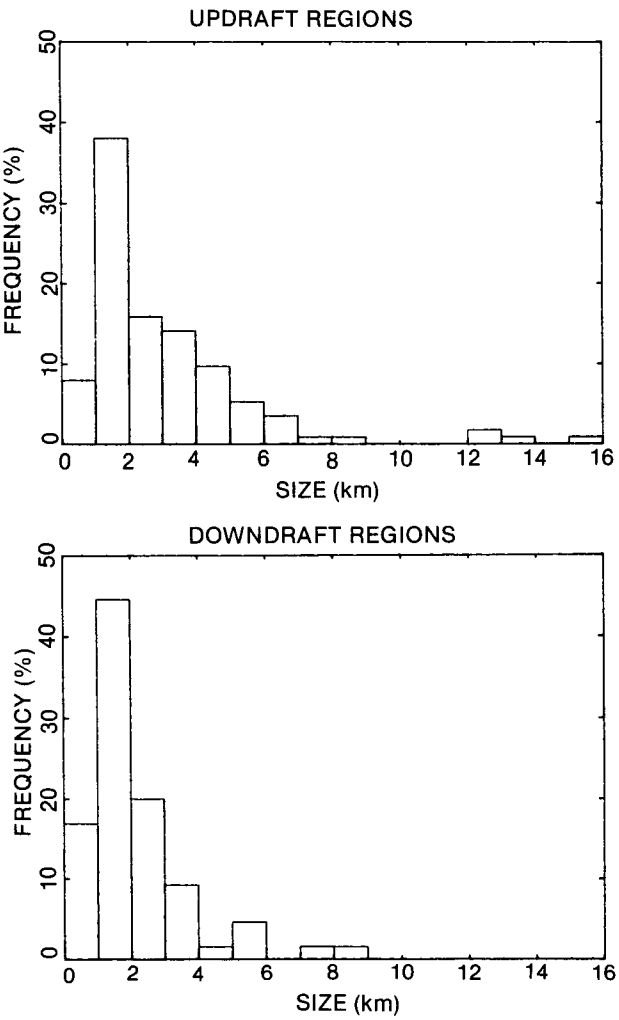

FIG. 4. Frequency distribution of updraft (top) and downdraft (bottom) widths from the T-28 CCOPE storm penetrations.

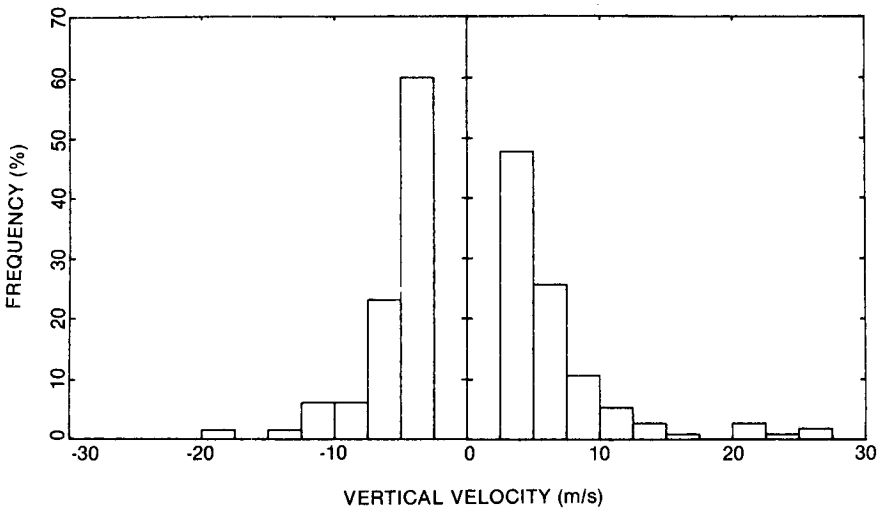

FIG. 5. Frequency distribution of the maximum updraft (right) and downdraft (left) speeds from the T-28 CCOPE storm penetrations. The 53 m s^{-1} updraft from the 2 August storm is offscale to the right.

The average updraft width was about 3 km, while the average downdraft size was about 2 km. These values are in rough agreement with those in Musil et al. (1977), who found using a similar selection scheme that the sizes of most updrafts and downdrafts in Colorado storms ranged from about 1 to 4 km. The Montana storms did contain updrafts as wide as 15 km, and downdrafts more than 8 km wide.

b. *Draft velocities*

Frequency distributions of the maximum vertical wind speed observed in each identified updraft–downdraft zone are shown in Fig. 5. The vertical velocities ranged between −18 and +53 m s^{-1}, with median speeds for the updrafts and downdrafts being about 5 and 4.5 m s^{-1}, respectively. The 53 m s^{-1} updraft (offscale in Fig. 5) from the 2 August storm (see Fig. 1) is a conspicuous outlier, indicating the unusual intensity of that storm. A weighted-mean vertical speed calculation based upon the sizes of the regions shows about 7 and 5.5 m s^{-1} for updrafts and downdrafts, respectively. The fact that updrafts tend to be stronger than downdrafts is a common observation (e.g., Musil et al. 1977; Knight and Squires 1982; Musil and Smith 1989).

There is some relationship between the updraft strength and observed size (Fig. 6). This should be expected because larger storms are generally more intense and tend to have stronger vertical motions. A considerably weaker relationship is found between downdraft size and speed. The updraft relationship appears to be stronger mainly because of the influence of several large, strong updraft regions occurring on 1 and 2 August 1981.

c. *Cloud water*

The cloud LWC in the vertical-draft regions was characterized by extreme variations from near zero to near adiabatic. Most LWC observations were substantially below adiabatic, except for the cores of a couple of updrafts that were sampled on 1 and 2 August. Over 40% of the draft regions contained very little cloud liquid. The observed maximum values in the updrafts were typically <25% of adiabatic, a behavior also noted in observations in the southeastern part of the United States (Musil and Smith 1989). The median of the ratio of average to peak LWC was about 0.5. A com-

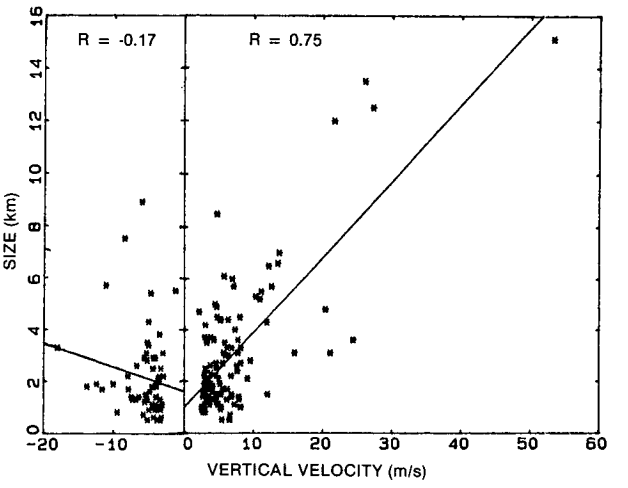

FIG. 6. Scatterplot and regression lines comparing the CCOPE draft sizes and maximum speeds. Correlation coefficient for the updrafts (right) is 0.75, while that for the downdrafts (left) is only −0.17.

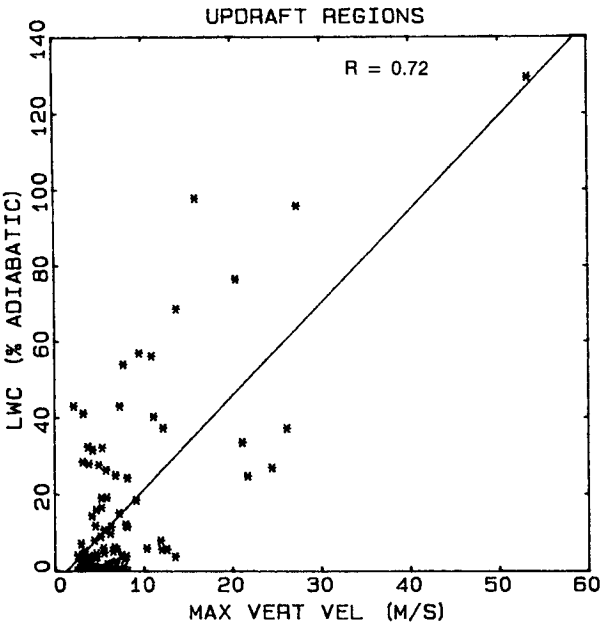

FIG. 7. Scatterplot and regression line comparing maximum cloud LWC in the CCOPE updraft regions (expressed as percent of the adiabatic values) with the maximum updraft speed.

parison (Fig. 7) between the maximum observed LWC in each updraft region, expressed as a percent of adiabatic, and the maximum updraft speed shows some correlation. The superadiabatic value in Fig. 7 occurred on 2 August, a case described in detail in Musil et al. (1986) and Miller et al. (1988).

Interestingly, downdrafts often contained substantial amounts of cloud liquid. In about 43% of the downdrafts (versus just 53% of the updrafts), the maximum LWC value exceeded 0.2 g m^{-3} (Fig. 8). A few downdrafts contained LWCs of more than 1 g m^{-3}. The ratios of observed to adiabatic LWC values were all less than 50%, but otherwise were generally similar to those found in updrafts; however, there was no correlation between these ratios and downdraft speed. The idea that the downdrafts are free of cloud water is not substantiated by these observations.

The specific reasons for the relatively low LWC values in the updrafts are not known. These were mature storms, and some combination of dilution by entrainment of dry air and depletion by larger particles may be involved. Instrument error may also play a role; the manufacturers for the JW device claim an accuracy of about ±20%. Using that as a guide, any ratio of peak cloud LWC to adiabatic greater than about 80% could represent an adiabatic core, but that only gives three to four cases. The observation of essentially adiabatic values in the two large storms suggests that instrument errors were not a major factor in the generally subadiabatic observations. It is also worth noting that even the possible adiabatic regions represent only extremely small portions of the entire updraft regions that were sampled (Musil et al. 1986). Information beyond just the observations by the T-28 would be required to make a complete investigation of this situation.

It is interesting that the two days (1 and 2 August) on which the largest and strongest updrafts were encountered during CCOPE were also the days with the highest ratios of observed to adiabatic LWC. This suggests that the wide updraft regions and high velocities could reduce the amount of mixing with environmental air, increasing the possibility for the existence of an adiabatic core. If this is true, there should be a relationship between peak LWC and updraft strength or size (or perhaps some combined measure such as the product of strength and size). The strongest correlation was found between peak LWC and peak updraft speed (Fig. 9), showing a general tendency for the LWC to increase as the updraft speed increases. However, the relatively high correlation coefficient of 0.87 is again largely influenced by the points for the same two storms mentioned above. Past work by Musil et al. (1977) yielded a lower correlation coefficient of 0.67 for a similar set of data gathered in northeast Colorado during the National Hail Research Experiment.

Another factor may be that the strong updrafts limit the time available for precipitation-particle growth and

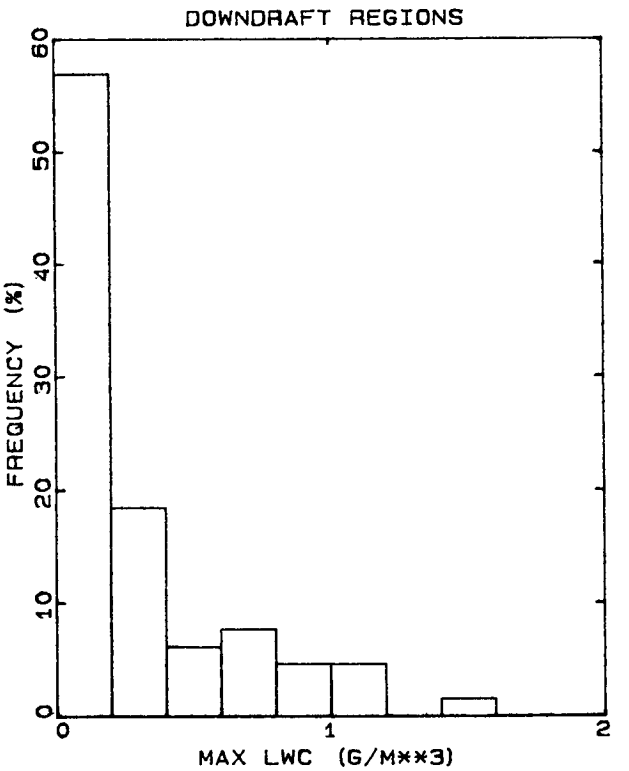

FIG. 8. Frequency distribution of maximum cloud LWC observed in the CCOPE downdrafts.

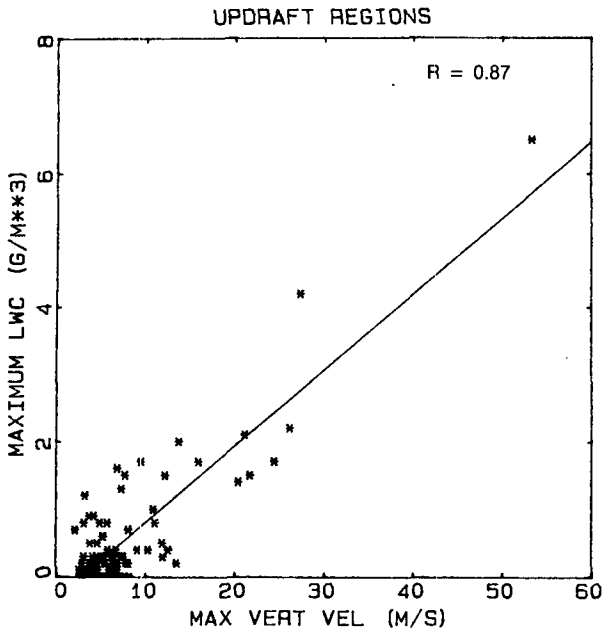

FIG. 9. Scatterplot and regression line comparing maximum cloud LWC in the CCOPE updraft regions with the maximum updraft speed.

hence restrict the LWC depletion. However, the hydrometeor observations on other storms with weaker updrafts do not show the presence of particles in sufficient quantities to deplete the cloud water significantly in updraft cores at the penetration levels. Consequently, dilution by entrainment appears to be the most plausible explanation for the observations, unless the depletion is active at some unobserved place in the storms. In some cases, the values of equivalent potential temperature provide clear indications of mixing effects (e.g., Musil et al. 1986; Kubesh et al. 1988).

d. Turbulence

Frequency distributions for maximum values of turbulent eddy dissipation rate in the CCOPE storms (Fig. 10) show that the intensity ranged from moderate to extreme (MacCready 1964). The updrafts tended to be somewhat more turbulent than the downdrafts. The highest value of about 21 $cm^{2/3}\ s^{-1}$ was found in an updraft, while the maximum value found in a downdraft region was 18 $cm^{2/3}\ s^{-1}$.

A comparison between the maximum vertical wind velocity and the peak turbulence in each updraft or downdraft region (Fig. 11) yields a correlation coefficient of about 0.70 in either case. Thus, there is also a good indication that more intense turbulence is associated with larger storms because the higher draft velocities tend to be found in larger storms. Because of the 8 s (or roughly 0.8 km) sampling interval used in the turbulence calculation, it is difficult to make very refining statements about the location of turbulence associated with the draft regions, especially the small ones. Generally, the most intense turbulence was randomly positioned with respect to the updraft regions. One exception was the first penetration on 2 August (Musil et al. 1986); those data showed an extremely large updraft in a well-organized storm, with strong turbulence along the edges of the updraft region and much less turbulence in the interior.

5. Features of the T-28 hail observations

a. General characteristics

The data from the hail spectrometer were first examined in conjunction with all the other data from the T-28 system to detect any irregularities. This led

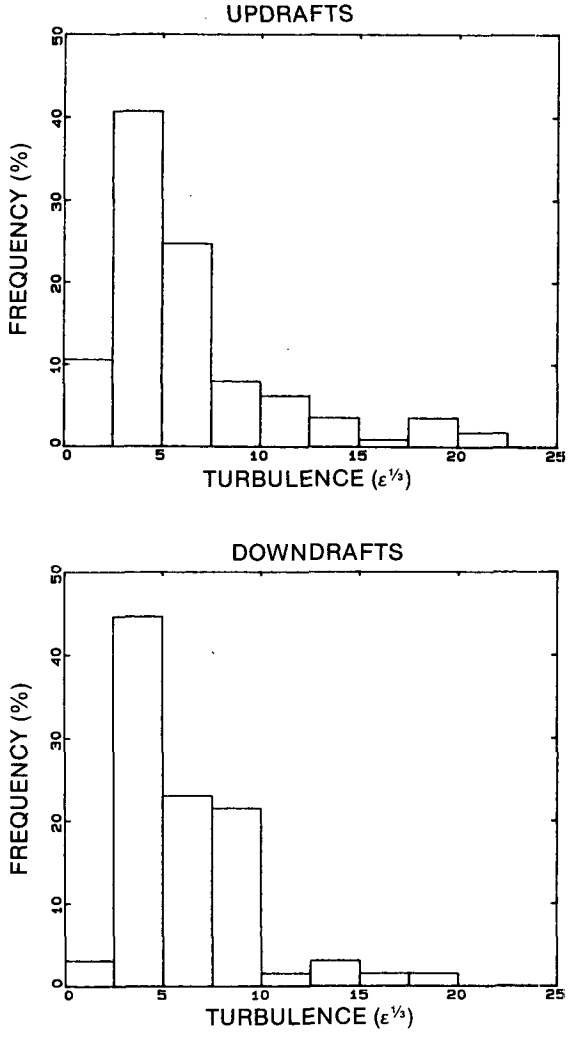

FIG. 10. Frequency distributions of the maximum turbulent eddy dissipation rate ($cm^{2/3}\ s^{-1}$) in the CCOPE updrafts (top) and downdrafts (bottom).

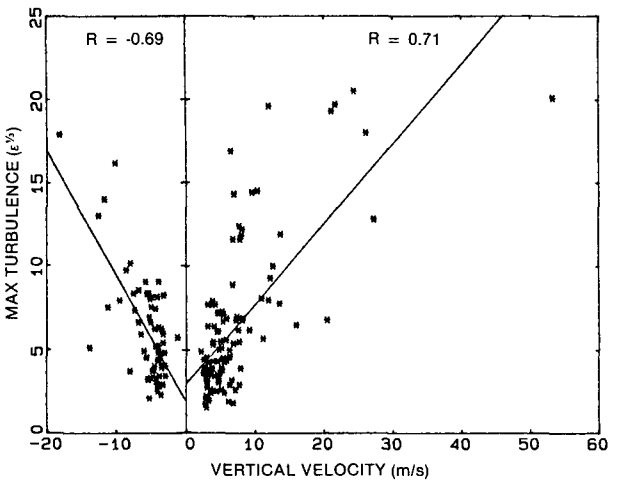

FIG. 11. Scatterplot and regression lines comparing the maximum turbulent eddy dissipation rate ($cm^{2/3}\ s^{-1}$) in the CCOPE draft regions with the corresponding maximum draft velocity. The correlation coefficient for updraft regions (right) is 0.71 and that for downdraft regions (left) is −0.69.

to the elimination of 22 July from the hail dataset because of erratic counts by the hail spectrometer, and 21 July was dropped because no hail counts were observed. However, data from 12 and 13 July were used in the hail analysis, although those days were not included in the determinations of the draft regions discussed in section 4.

Table 2 shows data from each storm penetration considered in the hail analysis. Included is a summary of the general characteristics of the hail observations, as well as the values of the maximum LWC and maximum updraft speed for each penetration.

The maximum hailstone size detected by the hail spectrometer on a penetration ranged over the full instrument working range of about 5–50 mm during the CCOPE field season. The greatest maximum size of 50 mm was observed in the 2 August supercell storm. Maximum hailstone number concentrations ranged up to 35 m^{-3}, observed during penetration 5 of the 29 July storm (a relatively weak storm in the stage of dissipation). The hail mass concentrations ranged up to about 12 g m^{-3}, which was also observed on 2 August. The maximum cloud LWC ranged up to 2.5 g m^{-3} except in the 1 and 2 August storms, where the LWC reached near-adiabatic values in the updraft cores. Penetrations in those storms exhibited strong updrafts of 25 m s^{-1} or more.

b. *Cases with large hail*

A more detailed analysis of the hail characteristics was performed for one storm (23 July) with large hail (see the Appendix). The results can be compared with previous detailed analyses from the 1 and 2 August storms (Musil et al. 1986; Kubesh et al. 1988). These three storms contained the largest hail encountered by the T-28 during CCOPE, and they also had the widest updrafts. Comparisons of the hail data from the three

TABLE 2. Summary of T-28 hail observations during CCOPE.

Flight	Date (1981)	Penetration number	Time In (MDT)	Time Out (MDT)	Maximum hail number concentration (m^{-3})	Maximum hail mass concentration (g m^{-3})	Maximum hail size (mm)	Maximum cloud LWC (g m^{-3})	Maximum updraft (m s^{-1})
327	12 July	1	1808:33	1814:41	5	1.0	11.0	2.5	—*
		2	1825:24	1830:21	10	5.0	18.0	2.0	—
		3	1838:03	1846:35	10	1.0	9.4	0.5	—
		4	1858:24	1906:00	10	1.0	7.0	1.0	—
328	13 July	1	2015:46	2023:14	10	2.0	9.4	1.0	—
		2	2024:46	2033:56	10	1.0	9.4	1.0	—
		3	2036:18	2041:32	1	0.1	6.0	2.5	—
		4	2046:42	2050:07	1	0.1	6.0	2.5	—
330	19 July	5	1500:11	1504:29	10	2.0	11.0	1.0	14
		6	1509:21	1514:18	10	1.0	11.0	1.0	5
334	23 July	1	1607:05	1612:22	20	5.0	26.1	1.5	12
336	29 July	3	2027:42	2030:31	4	0.5	13.0	0.3	7
		4	2033:44	2038:04	18	1.0	9.4	—	—
		5	2040:14	2044:13	35	3.5	15.6	—	—
		6	2047:01	2050:30	20	1.5	13.0	0.2	16
337	1 August	3	1648:18	1652:27	5	1.0	26.0	4.2	27
		4	1702:19	1705:21	2	0.1	18.6	0.8	5
338	2 August	1	1842:16	1852:59	30	8.0	50.0	6.5	53
		2	1912:11	1918:21	15	12.0	50.0	2.0	26
		3	1921:21	1932:53	8	5.0	50.0	1.5	25

* Blank indicates no observation was made.

TABLE 3. Summary of correlation coefficients for reflectivity gradient analysis.

Date	Penetration number	Hail concentration vs horizontal gradient	Hail concentration vs Z	Maximum diameter vs horizontal gradient	Maximum diameter vs Z	Maximum diameter vs hail concentration
1 August	3	0.02	0.48	−0.24	0.52	0.78
2 August	1	−0.26	0.83	−0.09	0.61	0.58
	2	−0.46	0.54	0.15	0.52	0.64
	3	0.00	0.76	0.15	0.60	0.64

model in a comparable gradient analysis for the 2 August case. The horizontal reflectivity gradient from the model output (the only one available is for the x axis) was compared with the simulated concentrations of ice particles > 5 mm, which corresponds to the lower size limit of the T-28 hail spectrometer. An inverse relationship between reflectivity gradient and hail concentration was also apparent in the model results. The model hail concentration showed a relationship with radar reflectivity similar to that in the observations, but the correlation coefficient from the model results was slightly lower. Thus, there is general agreement between these observations and 2D model results in regard to the relation of the hail to reflectivity and reflectivity gradient.

7. Summary and concluding remarks

Some of the interior characteristics at about the 6-km altitude of several southeastern Montana hailstorms have been presented. Part of the analysis concentrated on vertical drafts with horizontal dimensions greater than about 500 m and showed that about half of the updraft–downdraft regions were no wider than about 1.5–2.0 km. The largest updraft encountered was about 15 km wide, and the largest downdraft a little more than half as broad. Vertical winds ranged from about −20 to +50 m s^{-1}, with median updraft and downdraft speeds being about 5 m s^{-1}. Updraft speed showed moderate correlation with updraft size. The sizes and intensities of the vertical draft regions studied are quite similar to those found in other High Plains thunderstorms penetrated by the T-28.

Observations of cloud liquid water concentrations in the vertical draft regions were overwhelmingly subadiabatic, except in two very large, intense hailstorms. Even in those cases, the near-adiabatic regions represented only a small portion of the updraft regions. The observed peak LWC values in updrafts generally increased as the maximum updraft speed increased, but the actual observations of cloud LWC were extremely variable. Many of the downdraft regions also contained appreciable amounts of cloud liquid. Thus, particle trajectory and hailstone growth analyses in the various models that generally assume adiabatic liquid water concentrations in the updraft regions and zero in the downdrafts will most certainly be questionable. Knight and Knupp (1986) have shown in sensitivity tests that cloud LWC was the most important specification in their model. Our observations indicate that, if a fixed assumption is necessary, LWC values around 25% of adiabatic values would be nearer the mark.

The updrafts tended to have somewhat more intense turbulence. A modest correlation between maximum vertical wind speed and maximum intensity of turbulence in the draft regions was found. This confirms that, in a general sense, more extreme values of turbulence are associated with larger, more intense storms.

During CCOPE, the maximum hail number and mass concentrations observed with the T-28 ranged up to about 35 m^{-3} and 12 g m^{-3}. Maximum hailstone sizes encountered were about 50 mm. The hail was often found in regions of moderate updraft, and usually extended into an associated downdraft region to the east. Parts of the same updrafts (especially the western parts) were hail-free. The 2 August storm exhibited reverse behavior in that the eastern part of the updraft region was essentially hail-free, while the greatest amount of hail was found to the west of the WER. This difference may be a result of the intense circulations present in this supercell storm.

Whenever hail was encountered, the cloud LWC tended toward decidedly subadiabatic values and, in some cases (especially 2 August), was virtually nonexistent. Nevertheless, hail was found to coexist with substantial amounts of supercooled cloud water in parts of the updraft regions, especially near the updraft–downdraft boundary. This suggests that the hail encountered there was still in the process of growing by accretion, in conditions of subadiabatic LWC. This has implications for some of the hailstone growth models.

The vast majority of the hailstones encountered were probably falling against the updrafts observed. Larger hailstones tended to be found in storms with stronger updrafts, demonstrating again that strong updrafts are probably necessary to sustain the growth of large hailstones.

The largest hail encountered during CCOPE occurred in the three storms containing the widest updraft regions. This appears to be in agreement with findings

by Nelson (1983), who demonstrated that a critical factor for hail growth may be a broad region of moderate updraft, allowing more time for the development of hail. The storms on 1 and 2 August each had wide and intense updrafts, the one on 2 August being associated with a well-developed WER. Such a broad region of moderate updraft would be found around the periphery of the extremely strong updraft cores in those storms. Hail was indeed found in such peripheral updraft regions and the neighboring downdrafts. The parts of the storm penetrated on 23 July exhibited only moderate updrafts, but still had two of the wider updraft regions found in CCOPE. The process requiring a broad updraft is also related to the horizontal wind structure, which may influence the time that a particle resides in the updraft region of a storm.

Reflectivity gradients computed from the CP-2 radar data were compared with the hail observations made by the T-28 on 1 and 2 August. Results showed that the hailstone concentration was weakly and, if anything, inversely related to the reflectivity gradient. Hailstone concentration and maximum diameter correlated best with the reflectivity itself, thus demonstrating that hail in these storms is found in the high-reflectivity regions and not necessarily in high-reflectivity-gradient regions.

The observations presented in this paper provide information about the interior structures of hailstorms penetrated by the T-28 during the CCOPE field season. However, numerous questions concerning the hail-forming mechanisms of these storms still remain. Modeling techniques are a useful way of investigating these mechanisms. However, some models of hailstone growth may have serious problems because of differences between the specifications assumed in the models and the actual conditions in the clouds. For example, the cloud liquid water concentrations observed in updrafts seem to be considerably lower than the values assumed in many of the models. The downdrafts are often not free of cloud water, as is sometimes assumed. Furthermore, the problem of how well the Doppler radar data approximate the actual wind patterns in convective storms raises additional uncertainties in the results from growth–trajectory models.

The two-dimensional model of Farley and Orville (1986) does not produce growth trajectories for individual particles. However, by coupling the cloud dynamics and microphysics it develops the growth environment more realistically. For example, hailstones in the model generally grow in regions with LWC values less than half the adiabatic value. Downdrafts in the model often contain cloud water, in agreement with the observations reported here. Detailed comparisons of this model with observations from specific cases (e.g., Farley 1987; Kubesh et al. 1988) have shown generally favorable results.

The ever-changing conditions present in hailstorms almost defy complete specification and detailed understanding of the processes involved. The analysis of hydrometeor characteristics is very complicated; particle sizes, habits, and concentrations are the result of numerous and various growth trajectories within the storm environment. Certainly a more comprehensive hydrometeor description would be necessary to obtain a thorough understanding of the microphysical processes producing precipitation in these convective storms. The T-28 observations generally covered large regions of the storms in CCOPE, but at a single level. Most of the hail observed by the T-28 had originated elsewhere in the storms and much of it was still growing when encountered. The T-28 observations alone are not sufficient to determine the origin of the hailstones. The possibilities of melting and shedding suggested by Rasmussen and Heymsfield (1987) and the trajectory analysis work such as that by Miller et al. (1988, 1990) can be important clues. Remote sensing observations capable of distinguishing hydrometeor types (e.g., Bringi et al. 1983) can help to characterize a greater part of the storm's volume–time history.

On the basis of the T-28 observations, one is led to speculate that hail develops (and grows) in updraft regions having subadiabatic LWCs. This seems to occur primarily at the periphery of the virtually hail-free updraft cores. The process may proceed most rapidly above the CCOPE penetration level of the T-28. Finally, when the hail becomes large enough to fall against the updraft (perhaps loading it enough to diminish its strength), the descending mass works at depleting the available cloud water whether in updraft or downdraft.

Aircraft observations such as those reported here cannot, of themselves, provide enough information to produce complete answers to the questions about growth mechanisms. However, they can contribute to the database needed to analyze the processes of hail growth. The incorporation of these and other observations in the framework of suitably designed models offers the best hope of advancing our understanding of these mechanisms.

Acknowledgments. Support of this research was provided by the National Science Foundation under Grants ATM-8612385 and ATM-8720252, and Cooperative Agreement ATM-8620145. Acknowledgment is made to the National Center for Atmospheric Research Scientific Computing Division for part of the computer resources used in this research.

APPENDIX

Analysis of T-28 Hail Observations from 23 July 1981 CCOPE Storm

The T-28 made one penetration of the 23 July storm, on an eastbound heading at an altitude of about 6.2

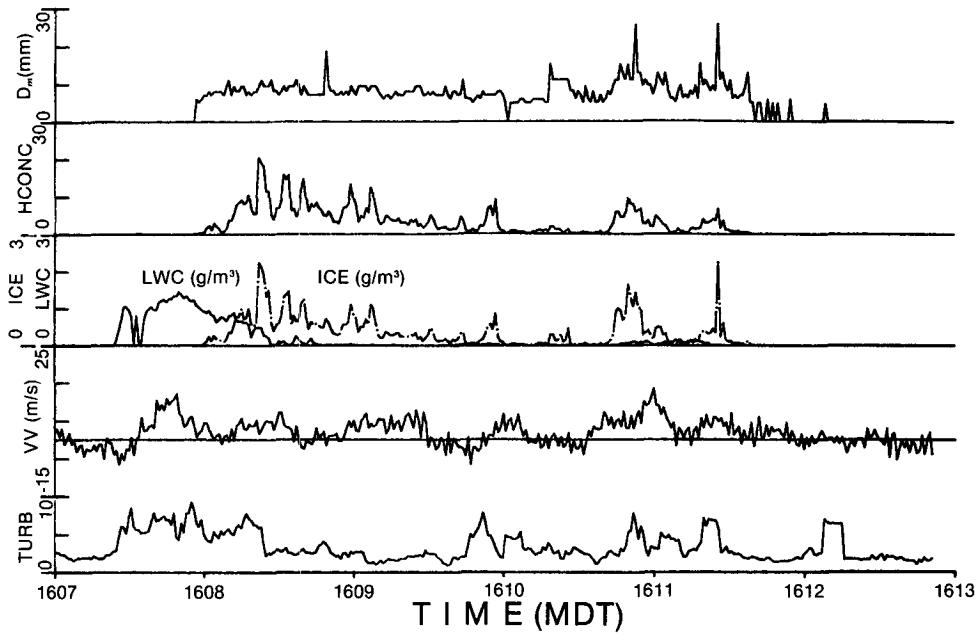

FIG. A1. Time plot of selected variables for the 23 June 1981 storm penetration. Top panel: maximum hailstone size (mm); second panel: hailstone concentration (m^{-3}); third panel: cloud LWC ($g\ m^{-3}$, solid line) and hail mass concentration ($g\ m^{-3}$, dash–dot line); fourth panel: vertical wind speed ($m\ s^{-1}$); bottom panel: turbulent eddy dissipation rate ($cm^{2/3}\ s^{-1}$).

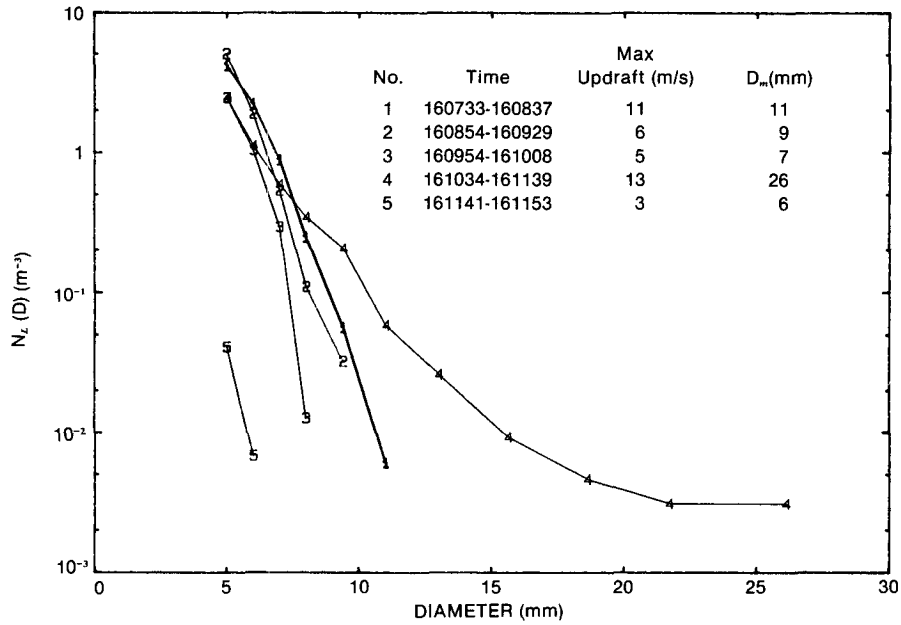

FIG. A2. Composite hailstone-size distributions for the five updraft regions identified from the 23 July penetration. Ordinate shows the number concentration (m^{-3}) of hailstones larger than the size indicated on the abscissa. The updraft time periods are (see Fig. A1): 1) 1607:33–1608:37; 2) 1608:54–1609:29; 3) 1609:54–1610:08; 4) 1610:34–1611:39; 5) 1611:41–1611:53 MDT.

km MSL (which corresponds to a temperature of about −16°C). The penetration was made several kilometers to the south of the high-reflectivity region (maximum, 56 dBZ), in a WER that was in the process of filling in. The reflectivity was rapidly increasing near the time of penetration. The exact position of the T-28 with respect to the storm reflectivity pattern is not known because only poor flight tracks were obtained on that day. However, the relationship of the hail to the reflectivity structure is not critical to the present discussion.

The sizes of the hailstones measured by the hail spectrometer ranged from about 5 to 26 mm (Fig. A1). The largest hailstones were found near the end of the penetration, in a major updraft region on the east side of the storm (1610:34–1611:39 MDT), although some hail was found throughout nearly the entire penetration. This updraft had a peak speed of about 13 m s^{-1}. Another major updraft region of similar size (about 6.5 km wide) and strength was encountered about 15 km to the west early in the penetration (1607:33–1608:37 MDT). It was virtually hail-free in the western part, but 1-cm hailstones and the highest hailstone number concentration (about 20 m^{-3}) were found on the east side. The hail mass concentration did not exceed about 3 g m^{-3} throughout the penetration. Hailstone number concentrations were lower in the eastern major updraft, but the mass concentrations were similar.

There was some cloud liquid through most of the westernmost updraft, but very little over the rest of the penetration. The cloud LWC peaked at about 1.5 g m^{-3} early in the penetration, near the first updraft peak. In the eastern part of the westernmost updraft, hail coexisted with substantial amounts of supercooled cloud water. This suggests that the hail encountered by the T-28 was still in the process of growing by accretion. The absence of significant cloud liquid in other regions of the penetration suggests that the hailstones encountered there were no longer growing rapidly. However, their earlier growth may have been a factor in depleting the cloud water in those regions.

The hailstone-size distributions were examined using the inverse cumulative number concentration plotting method described in Smith (1982). Plots showing the number concentration of hailstones larger than any given size were prepared for five updraft regions identified in this penetration (Fig. A2). There is no distinct separation among the distributions at the small end of the spectrum, except for the minor easternmost updraft designated as number 5. The two major updraft regions mentioned above had larger hailstones than the other, weaker updraft regions. The distribution from the western major updraft region (number 1) plots as a relatively straight line, indicating an exponential size distribution on this semilog scale. The one from the eastern major updraft (number 4) has a distinctive break in slope around 1.5 cm, similar to an observation made by Smith and Jansen (1982) from data gathered in an Oklahoma storm. No explanation for this observation is available at this time. The downdraft regions in this penetration were very small and contained no sizable hail.

REFERENCES

Auer, A. H., Jr., and W. Sand, 1966: Updraft measurement beneath the base of cumulus and cumulonimbus clouds. *J. Appl. Meteor.*, **5**, 461–466.

——, and J. D. Marwitz, 1972: Hail in the vicinity of organized updrafts. *J. Appl. Meteor.*, **11**, 748–752.

Baumgardner, D., W. Strapp and J. E. Dye, 1985: Evaluation of the forward scattering spectrometer probe. II: Corrections for coincidence and dead-time losses. *J. Atmos. Oceanic Technol.*, **2**, 626–632.

Bringi, V. N., V. Chandrasekhar, T. A. Seliga, P. L. Smith and R. Hari, 1983: Analysis of differential reflectivity (Z_{DR}) radar measurements during the Cooperative Convective Precipitation Experiment. Preprints, *21st Conf. Radar Meteorology,* Edmonton, Canada, Amer. Meteor. Soc., 494–499.

Christopher, S. A., 1989: T-28 hail observations and radar characteristics of Montana thunderstorms. M.S. thesis, Dept. of Meteorology, South Dakota School of Mines and Technology, Rapid City, 99 pp.

Cooper, W. A., 1978: Cloud physics investigations by the University of Wyoming in HIPLEX 1977. Rep. No. AS119, Dept. of Atmospheric Science, University of Wyoming, Laramie, 320 pp.

Dennis, A. S., and D. J. Musil, 1973: Calculations of hailstone growth and trajectories in a simple cloud model. *J. Atmos. Sci.*, **30**, 278–288.

Dye, J. E., and W. Toutenhoofd, 1973: Measurements of the vertical velocity of the air inside cumulus congestus clouds. Preprints, *Eighth Conf. Severe Local Storms,* Chicago, Amer. Meteor. Soc., 33–34.

Farley, R. D., 1986: Simulation of the 2 August 1981 CCOPE hailstorm. *Proc. First Int. Cloud Modeling Workshop Conf.,* Irsee, FRG, World Meteor. Organ., 99–110.

——, 1987: Numerical modeling of hailstorms and hailstone growth: Part II. The role of low density riming growth in hail production. *J. Climate Appl. Meteor.*, **26**, 234–254.

——, and H. D. Orville, 1986: Numerical modeling of hailstorms and hailstone growth. Part I: Preliminary model verification and sensitivity tests. *J. Climate Appl. Meteor.*, **25**, 2014–2035.

Foote, G. B., 1984: A study of hail growth utilizing observed storm conditions. *J. Climate Appl. Meteor.*, **23**, 84–101.

Heymsfield, A. J., 1982: A comparative study of the rates of development of potential graupel and hail embryos in High Plains storms. *J. Atmos. Sci.*, **39**, 2867–2897.

Johnson, G. N., and P. L. Smith, Jr., 1980: Meteorological instrumentation system on the T-28 thunderstorm research aircraft. *Bull. Amer. Meteor. Soc.*, **61**, 972–979.

Kelly, T. J., and D. H. Lenschow, 1978: Thunderstorm updraft velocity measurements from aircraft. Preprints, *Fourth Symp. Meteor. Observations and Instrumentation,* Denver, Amer. Meteor. Soc., 474–478.

Knight, C. A., 1982: The Cooperative Convective Precipitation Experiment (CCOPE), 18 May–7 August 1981. *Bull. Amer. Meteor. Soc.*, **63**, 386–398.

——, and P. Squires, 1982: *Hailstorms of the Central High Plains. Vol. I: The National Hail Research Experiment.* Colorado Associated University Press, 282 pp.

——, and K. Knupp, 1986: Precipitation growth trajectories in a CCOPE storm. *J. Atmos. Sci.*, **43**, 1057–1073.

Kopp, F. J., 1985: Deduction of vertical motion in the atmosphere from aircraft measurements. *J. Atmos. Oceanic Technol.*, **2,** 684–688.

Kubesh, R. J., D. J. Musil, R. D. Farley and H. D. Orville, 1988: The 1 August 1981 CCOPE storm: Observations and modeling results. *J. Appl. Meteor.*, **27,** 216–243.

Lenschow, D. H., 1976: Estimating updraft velocity from an airplane response. *Mon. Wea. Rev.*, **104,** 618–627.

MacCready, P. B., Jr., 1964: Standardization of gustiness values from aircraft. *J. Appl. Meteor.*, **3,** 439–449.

May, E. L., 1974: Analysis of foil impactor data from armored aircraft penetrations of hailstorms. M.S. thesis, Dept. of Meteorology, South Dakota School of Mines and Technology, Rapid City, 66 pp.

Miller, L. J., J. E. Dye and B. E. Martner, 1983: Dynamical–microphysical evolution of a convective storm in a weakly sheared environment. Part II: Airflow and precipitation trajectories from Doppler radar observations. *J. Atmos. Sci.*, **40,** 2097–2109.

——, —— and C. A. Knight, 1988: Airflow and hail growth in a severe northern High Plains supercell. *J. Atmos. Sci.*, **45,** 736–762.

——, J. D. Tuttle and G. B. Foote, 1990: Precipitation production in a large Montana hailstorm: Airflow and particle growth trajectories. *J. Atmos. Sci.*, **47,** 1619–1646.

Mohr, C. G., L. J. Miller, R. L. Vaughn and W. Frank, 1986: The merger of mesoscale datasets into a common Cartesian format for efficient and systematic analyses. *J. Atmos. Oceanic Technol.*, **3,** 144–161.

Musil, D. J., 1970: Computer modeling of hailstone growth in feeder clouds. *J. Atmos. Sci.*, **27,** 474–482.

——, 1971: Reply. *J. Atmos. Sci.*, **28,** 294–295.

——, 1972: Corrigendum. *J. Atmos. Sci.*, **29,** 225.

——, and P. L. Smith, 1989: Interior characteristics at midlevels of thunderstorms in the southeastern United States. *Atmos. Res.*, **24,** 149–167.

——, ——, J. R. Miller, Jr., J. H. Killinger and J. L. Halvorson, 1977: Characteristics of vertical velocities observed in T-28 penetrations of hailstorms. Preprints, *Sixth Conf., Inadvertent Weather Modification,* Champaign–Urbana, IL, Amer. Meteor. Soc., 166–169.

——, A. J. Heymsfield and P. L. Smith, 1986: Microphysical characteristics of a well-developed weak echo region in a High Plains supercell thunderstorm. *J. Climate Appl. Meteor.*, **25,** 1037–1051.

Nelson, S. P., 1983: The influence of storm flow structure on hail growth. *J. Atmos. Sci.*, **40,** 1965–1983.

Paluch, I. R., 1978: Size sorting of hail in a three-dimensional updraft and implications for hail suppression. *J. Appl. Meteor.*, **17,** 763–777.

Peterson, B. A., 1989: Hydrometeor characteristics in COHMEX thunderstorms as derived from computerized reduction of foil impactor data. M. S. thesis, Dept. of Meteorology, South Dakota School of Mines and Technology, Rapid City, 69 pp.

——, D. J. Musil and P. L. Smith, 1990: Computerized reduction of airborne foil impactor data from COHMEX thunderstorms. Preprints, *Conf. Cloud Physics,* San Francisco, Amer. Meteor. Soc., 352–355.

Rasmussen, E. N., and R. B. Wilhelmson, 1983: Relationships between storm characteristics and 1200 GMT hodographs, low-level shear and stability. Preprints, *13th Conf. Severe Local Storms,* Tulsa, OK, Amer. Meteor. Soc., 55–58.

Rasmussen, R. M., and A. J. Heymsfield, 1987: Melting and shedding of graupel and hail. Part III: Investigation of the role of shed drops as hail embryos in the 1 August CCOPE* severe storm. *J. Atmos. Sci.*, **44,** 2783–2803.

Sand, W. R., 1976: Observations in hailstorms using the T-28 aircraft system. *J. Appl. Meteor.*, **15,** 641–650.

——, J. L. Halvorson and T. G. Kyle, 1976: Turbulence measurements inside thunderstorms used to determine diffusion characteristics for cloud. *Proc. Second World Meteorological Organization Conf. on Weather Modification,* Boulder, 539–545.

Shaw, W. S., 1974: Development of an airborne optical hailstone disdrometer. M. S. thesis, Dept. of Meteorology, South Dakota School of Mines and Technology, Rapid City, 40 pp.

Smith, P. L., 1982: On the graphical presentation of raindrop size data. *Atmos. Ocean,* **20,** 4–16.

——, and D. C. Jansen, 1982: Observations inside SESAME thunderstorms with an airborne hail spectrometer. Preprints, *12th Conf. Severe Local Storms,* San Antonio, Amer. Meteor. Soc., 16–19.

Stith, J. L., D. A. Griffith, R. L. Rose, J. A. Flueck, J. R. Miller, Jr. and P. L. Smith, 1986: A preliminary study of transport, diffusion, and ice activation in cumulus clouds using an atmospheric tracer. *J. Climate Appl. Meteor.*, **25,** 1959–1970.

Telford, J. W., P. B. Wagner and A. Vaziri, 1977: The measurement of air motion from aircraft. *J. Appl. Meteor.*, **16,** 156–166.

Weisman, M. L., and J. B. Klemp, 1982: The dependence of numerically simulated convective storms on vertical wind shear and buoyancy. *Mon. Wea. Rev.*, **110,** 504–520.

——, and ——, 1984: The structure and classification of numerically simulated convective storms in directionally varying wind shears. *Mon. Wea. Rev.*, **112,** 2479–2498.